

# Measuring surface water in soil with light reflectance.

Michael L. Whiting\*

Center for Spatial Technologies and Remote Sensing,  
Department of Land Air Water Resources, University of California, Davis

## ABSTRACT

The light absorbed by water in soil and plants is readily determined using hyperspectral full-range imagery and field spectrometers. The full absorption of light can be accounted for by fitting the shape of water absorptions at the same time as other diagnostic bands using multiple Gaussian functions. This research is particularly important in soils due to the loss of mineral band depth with the spread of the fundamental water just beyond the SWIR. The relationship of the albedo lost to band depth, for the same mineral media, is nonlinear. By including water and mineral absorptions in the same fitting, the accuracy of the mineral abundance estimates are shown substantially improved. In addition, measurements of absorption change within the soil surface are so sensitive to water content that these bands as indexes and absorption fitting are excellent predictors of the amount of organic matter. Spectral model is shown for determining water content based water indexes and the fitted SWIR band as a good predictors of soil biological crust, such as lichen and cyanobacteria, in hyperarid soils of the Mojave Desert.

## Keywords:

soil, soil-water, water absorption, mineral absorption, water thickness

## 1. INTRODUCTION

Within the ultra-violet (~ 200 nm) through the visible (350 to 700 nm), near-infrared (700 to 1200 nm) and shortwave infrared (1200 to 2500 nm) to beyond 3000 nm water absorbs light in broad bands that widen with increasing water content that mask adjacent mineral bands, and thus diminish the absorption depths of minerals and organic matter in soil. Techniques that utilize band depths as a means of determining mineral abundance are susceptible to error due to these water light absorptions. Water and soil particles are intimately mixed when below field capacity (i.e., after the macro pore are drained) and spectral measurements of the water band depths have a non-linear relationship to water content. Understanding this relationship of water and solid soil particles leads to improving the accuracy of the mineral abundance and organic matter measurements.

Soil is an important background component in vegetation indexes and radiative transfer models. Variation in moisture and soil albedo impact the indexes, particularly NDVI<sup>[1]</sup>, and later improved with SAVI<sup>[2]</sup> and other indexes. In developing radiative transfer modeling, the soil line demonstrates incorporating the albedo change<sup>[3]</sup>. Early attempts have included water content parameters in soil spectrum models and inverted the model to determine water content and other broad absorptions<sup>[4]</sup>.

### 1.1 Chromophores

Baumgardner et al., Henderson et al., and Stoner et al.<sup>[5-7]</sup> describe the major constituents in soils that give the colors and light reflectance intensity. Stoner et al.<sup>[7]</sup> determined from studying spectra from 239 soil series from around the United States that the primary chromophores in soil are water, clay, organic matter and iron contents. In the visible (400 to 700 nm), organic matter and iron are the principal light absorbers in soils, with water and clay mineral absorbs in the shortwave infrared region. Bowers and Hanks<sup>[8]</sup>, in a sequence of moisture contents, demonstrated the loss of albedo with increase water content, and non-linear change. Idso et al.<sup>[9]</sup> in early attempts to quantify the soil moisture level in agricultural fields used radiometer measurements to estimate water content. Attenuation of the EMF by water within specific regions is also a means of determining an equivalent water thickness, whether at the micron scale of soil spectroscopy or satellite imagery at the cropland scale<sup>[10, 11]</sup>. Of course, due to the short attenuation in the optical region tells us little of the below surface water contents, and without exposing the soil at depth to the spectrometer will not

\*email: mwhiting@ucdavis.edu; webpage: www.cstars.ucdavis.edu

replace in-place sensors for measuring water content with depth<sup>[12]</sup>. Other regions in the EMR provide the means to measure moisture with depth including thermal infrared, and radar with greater depth of attenuation.

### 1.2 Intimate mixtures-soil and water

At the scale of photons and material interactions, the water and solid particles are not spatially separable, the photons are reflected, refracted, and absorbed by these components within the radiative path. The electronic bonds within the solid phase and water are intimately mixed, thus the amount of light absorbed is non-linear to the contents of the water and minerals<sup>[13]</sup>. The regions of light absorbed by metal-OH and HOH are different, but generally very close together due to bond type. The strong hydrophilic nature of clay and organic matter increases the difficulty of quantifying the solid phase.

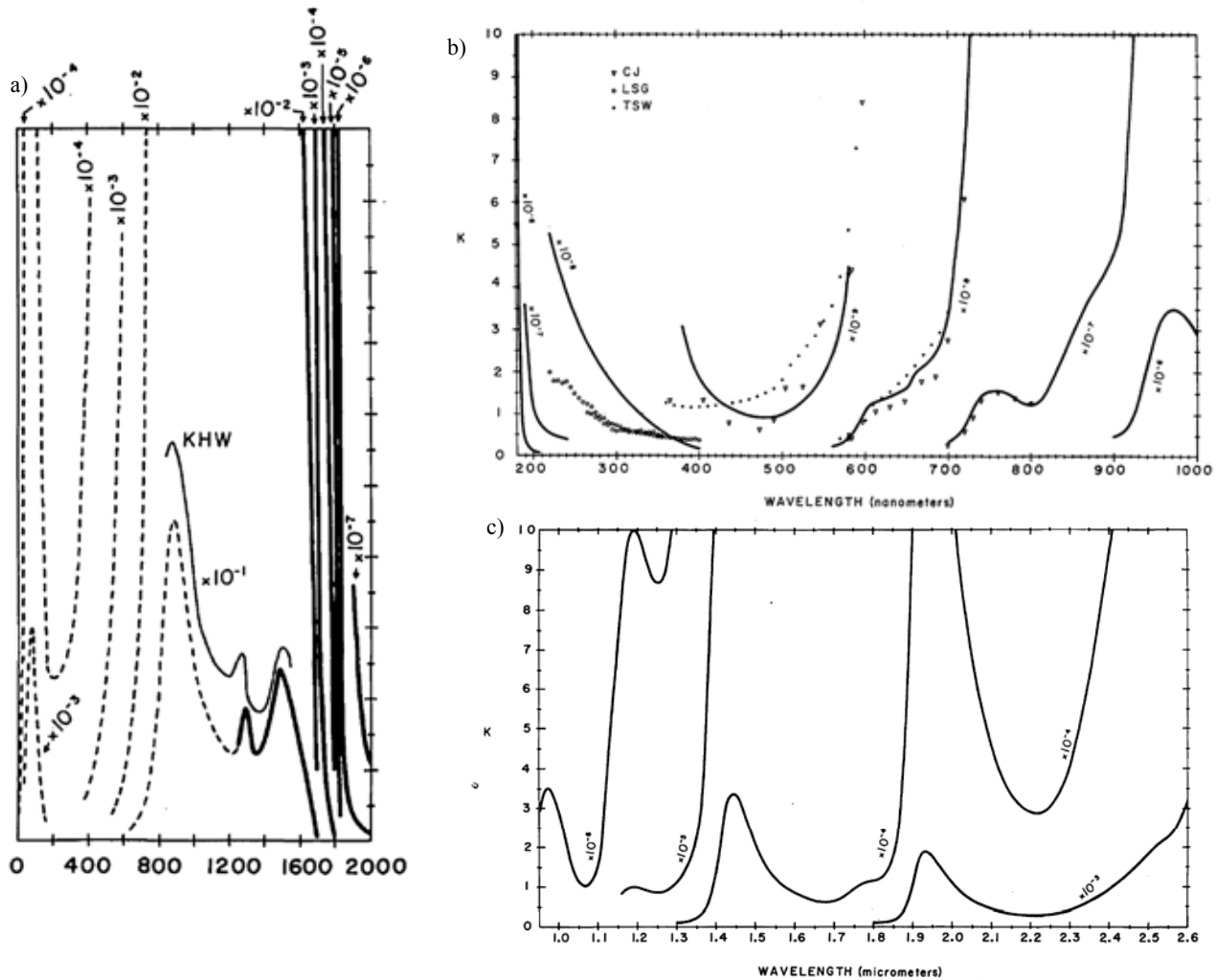


Fig.1 a) Water extinction coefficients below 200 nm (shown in Angstroms); b) coefficients between 200 to 1000 nm; c) coefficients 1000 to 2600 nm (shown in micrometers).<sup>[16]</sup>

For an excellent review of soil and water reflectance properties the reader is referred to Ben-Dor et al.<sup>[14]</sup>. They separate soil water into three parts: hydration water within the mineral lattice; hygroscopic water adsorbed on the particle surface; and free water in the macro pores. Water has three fundamental absorptions with the OH bond a) symmetric stretching  $\nu_{w1}$ ; b) bending  $\delta_w$ ; and c) asymmetric stretching  $\nu_{w3}$ . The combinations of these vibrations of OH generate diagnostic absorptions at 950 nm ( $2\nu_{w1} + \nu_{w3}$ ); 1200 nm ( $\nu_{w1} + \nu_{w3} + \delta_w$ ); and 1400 nm ( $\nu_{w3} + 2\delta_w$ ), and 1900 nm ( $\nu_{w3} + \delta_w$ ), in order of strength from very weak to very strong.

### 1.3 Endmember absorptions

Generally, water absorption features are thought of at 970, 1240, 1400, and 1900 nm within the remote sensing community due to the range of our instruments. Important absorptions spread occur in the visible region due to water in the UV and in the SWIR at wavelengths beyond the instrument limits<sup>[15]</sup>. Later we show that modeling with these absorptions beyond the instrument range improves the mineral abundance estimates. Pure water extinction coefficients were gathered from fifty-eight articles and books from 1892 to 1973 shows these strong absorption in 180 to 200 nm and 3000 nm regions (Fig. 1)<sup>[16]</sup>.

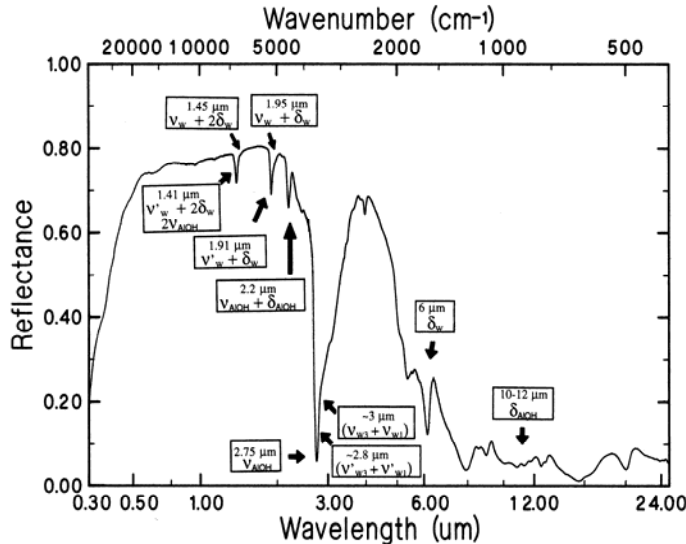


Figure 2. Combination and overtones of water stretching ( $\nu$ ) and bending ( $\delta$ ) absorptions in the bound ( $\nu'_w$ ) and adsorbed water ( $\nu_w$ ) vibration in association with Al-OH bonds of this montmorillonite clay ( $\nu_{AlOH}$ )<sup>[17]</sup>, copyright *Clay and Clay Minerals*.

The principal regions of hydroxyl bond (OH) bend and vibration light absorption varies with the ligand and metal interactions, and position within the clay lattice. Within a purged environment the particle surface water can be removed to resolved the absorbed from adsorbed water band centers. With montmorillonite clay, Bishop et al.<sup>[17]</sup> determined water that was absorbed (bound) within the mineral plates as 1410 nm ( $\nu'_w + 2\delta_w$ ;  $\nu_{AlOH}$ ) and 1910 nm ( $\nu'_w + \delta_w$ ) compared to ambient atmosphere water adsorbed (surface water) band centers closer to those of pure water at 1450 nm ( $\nu_w + 2\delta_w$ ) and 1950 nm ( $\nu_w + \delta_w$ ) seen in Fig. 2. Care must be taken in eliminating the water for determining the mineral under regulated humidity<sup>[17]</sup>. Harsh high temperature removal of the water can also reconstruct the solid phase<sup>[18]</sup>.

Fortunately, the hydroxyl at the edge and interior of clay and slit size minerals in soils absorb light at sufficiently different regions that allows to quantify the mineral type and abundance<sup>[13, 19-21]</sup>, and are between the strong 1900 nm and 2800 nm

absorptions of water. For example, kaolinite and montmorillonite diagnostic bands are at 2100 and 2200 nm, though this varies slightly with the interstitial mixture of cations. Organic constituents of soil, principally for starch, lignin and cellulose are assigned regions at 1700, 2100, and 2350 nm in the SWIR and a very broad absorption in the visible region from 500 to 700 nm<sup>[22]</sup>.

### 1.4 Quantifying water content

In evaluating soil water content, the thickness of the moist soil sample is an important consideration. With limited optical penetration the surface must be representative of the overall water content that is weight or pressurized. A highly accurate optic method of determining the water content may in the end be a better measure of water content with the thin surface for analyzing on soil phase analysis.

Gravimetric determination of water content in soil is the most common method. Moist samples are weighed before drying and reweighed after driving off the water. The difference in weight divided by the weight of the dry soil is the water fraction or with multiplying by 100 is the percentage<sup>[23]</sup>. The volumetric water content is generally calculated from the weigh change in a known sample volume by using an estimate of solid phase particle density (ca 2.69 gcm<sup>-3</sup>) and the density of water (1 gcm<sup>-3</sup>)<sup>[23]</sup>. There are errors introduced by particle density, especially with volcanic and organic soils. Volumetric estimates are also susceptible to errors in small samples due to changes in volume of soil pore and swell of some clay types as water content changes before and after wetting.

Where the application is directed towards plant water uptake, the soil spectral measurements have been related directly to the soil matrix (osmotic) potential to hold water against pressure, reported in mega Pascals (MPa) or Bars of negative pressure. Within a chamber, thin samples, less than 0.5 cm, are moistened on ceramic plates then with increasing

pressure in the chamber, the water is extracted until at equilibrium with the internal pressure<sup>[23]</sup>. Reflectance is measured through a sequence of these pressures.

### **1.5 Soil spectroscopy: Measurement the quantitative and the qualitative approaches.**

The differences in soil color and tone due to variation in water, secondary clay mineral and organic matter content in aerial photography has been an early use in soil survey and other inventories. Now with digital imagery, Persson et al.<sup>[24]</sup> demonstrated the albedo effect of water on soil by regression model of Saturation and Value (HSV converted RGB imagery) to predict water contents ( $r^2 = 0.99$ ) for natural loam, sandy loam, loamy sand, and pure silica fine sand, with low soil organic matter (SOM). They also saw that beyond saturation, the reflectance turns specular and the albedo brightens. Post et al.<sup>[25]</sup> at two moisture levels air and wet (but not glistening) was able to invert the color relationship to predict albedo (300 to 2800 nm) from the Munsell color (particularly color value,  $r^2 = 0.93$ ) of 26 soils of a broad range of texture and colors.

Determining soil moisture content in the visible-SWIR region in remote sensed images<sup>[26-28]</sup>. The position of these water bands support the adoption of water indexes generated for vegetation, such Normalized Difference Water Index (NDWI)<sup>[29]</sup> and Moisture Stress Index (MSI)<sup>[30]</sup>. On a quantitative basis, this indicates an influence of water on the soil lines for different soils, which agrees with Baret et al.<sup>[31]</sup>.

Early work in correlating soil moisture content to spectral measurements was made by individual bands using derivatives, PCA or other chemometric statistics. Five and seven water bands have been found to estimate water content<sup>[31, 32]</sup>; wavelengths of 1926, 1954, and 2150 nm<sup>[33]</sup> have also been suggested. Demattê et al.<sup>[34]</sup> used regression models for predicting the water content based on band depths at 1400, 1900, and 2200 nm for various tropical soils. The absorption features observed for clay patterns were helpful to characterize soil mineralogy. Variation in these bands is a function of texture and organic matter constituents. When measured directly, the soil water potential is inversely related to water content, i.e., increases negative pressure as the albedo increases. Baumgardner et al.<sup>[5]</sup> demonstrated with the loss of albedo so does the band depth diminish at 1400 and 1900 nm, same as Bowers and Hanks<sup>[8]</sup> found for gravimetric water content. Some investigators have determined water content not in relation to the dry weight of soil, but as related to saturation. Liu et al.<sup>[31, 32]</sup> regression models for predicting volumetric water content based on bands found through PCA, as did Lobell and Asner<sup>[35]</sup> related saturation ratio as a function of several band depths.

With the spectral shape of the water absorptions, there are a number of measurements that can be correlated to the water content. Simple continuum removal and band depth (BD)<sup>[36]</sup> is the most direct measurement. Milliken and Mustard<sup>[18]</sup> used BD determined by iteration of straight lines over the absorptions between local maxima until points along the continuum are  $\leq 1$ . The integration of the BD (IBD) and band area (IBA) are the sum of the band depths at each measured wavelength and integrated area within the band of interest.

Counter to previous general studies, Milliken and Mustard<sup>[37]</sup> study of monomineralic montmorillonite, Mg-exchanged montmorillonite, palagonite, clinoptilolite, and MgSO<sub>4</sub>·nH<sub>2</sub>O determined band depths within the SWIR (1.9  $\mu$ m) did not provide highly correlated general regression model to water content (between 0 and 20 %), however, on a mineral by mineral basis water was correlated. They also found the BD at the fundamental near 2800 nm was highly predictive of the water content among all samples, and was improved with Single-scatter albedo transformed spectra. Whiting et al.<sup>[38]</sup> found in a broad range of soil textures and carbonate contents the depth and area of the Gaussian absorption of the 2800 nm absorption were better predictors than the width at the point of inflection (one standard deviation).

The first principles of water absorption and light attenuation can be used to predict the thickness and relate this to the amount of water. Milliken and Mustard<sup>[37, 39]</sup> and Mulla et al.<sup>[40]</sup> have shown correlations light absorption with water film thickness.<sup>[18]</sup> also evaluated the Mean optical Path Length (MOPL) is an estimate of the thickness of the mineral or water based on the absorption and reflectance from the imaginary index of refraction of bulk water from lab determinations. The normalized optical path length (NOPL) is calculated similarly by adding the difference of the continuum from 1 (to increase the reflectance of the band) then dividing (normalizing) by this difference. This normalization increased sensitivity in regions with very high absorptions by other components than water (low continuum values).

## 2. SOIL SPECTRAL APPLICATIONS INCORPORATING WATER CONTENT

### 2.1 In the laboratory

Air dry soil samples exposed to ambient conditions will absorb moisture from the atmosphere, and depending on the amount and type of clay can hold 4 to 8 % water (gravimetric). Low temperature (30 °C) oven drying will reduce the water content without modifying the mineral and organic matter content. However, when removed from the oven, it is necessary to immediately put in a desiccator to continue the drying and prevent change. If the reflectance measurements are taken in an ambient air system, the soil will immediately begin to absorb moisture, and this is apparent when multiple reflectance measurements are observed over several minutes. Accurate consistent spectral measurements are made in an enclosed system, purged of moisture for dry soils<sup>[17]</sup>. This system is elaborate and less applicable to field and image spectral analysis. Knowing there is moisture and including an indicator of the amount is one means of reducing the impact on the solid phase analyses. Presented are two investigations into the sensitivity of analyses using the water bands, including the fundamental water absorption at the upper limit of common field and airborne instruments.

### 2.2 Integrating water absorptions into multiple absorption fitting algorithm.

University of California, Davis investigators are assisting wine grape growers in the Lodi region, just south of Sacramento, California, USA, with increased precision of the application of potassium by mapping the general soil regions effected by potassium fixation. Due to variation in the soil minerals, some fields and portions of fields are deficient in the nutrient, elsewhere there is abundance in localized areas. In wine grapes, insufficient potassium uptake will reduce juice yield, and over fertilization will reduce juice quality<sup>[41]</sup>.

One cause of this variation is associated with the abundance of vermiculite mineral in the soil formed in the sediments from the Sierra Nevada Mountain range to the east. While the identification of the age and development of the soils is essential to understanding the potassium fixation distribution, within the soil regions there is significant variation in potassium availability. Our investigations were related spectral measurements to the amount of vermiculite and

potassium fixation for later use in detail soil mapping with airborne hyperspectral imagery. As our collaborators described the soils in pits and sampled for x-ray diffraction analysis and potassium fixation, we collected spectral measurements from the surface and pit faces, and from the lab air dried samples prepared for x-ray analysis.

Thirteen different soil series were sampled using horizon and depth collection method with a total of 16 pits and 115 soil samples collected in 2006. An estimated 71 sites were sampled in 2007. Since the x-ray diffraction (XRD) and potassium fixation analyses<sup>[42]</sup> were incomplete at the time of this report only twenty nine representative soil samples were analyzed from the 2006 and 2007 field season.

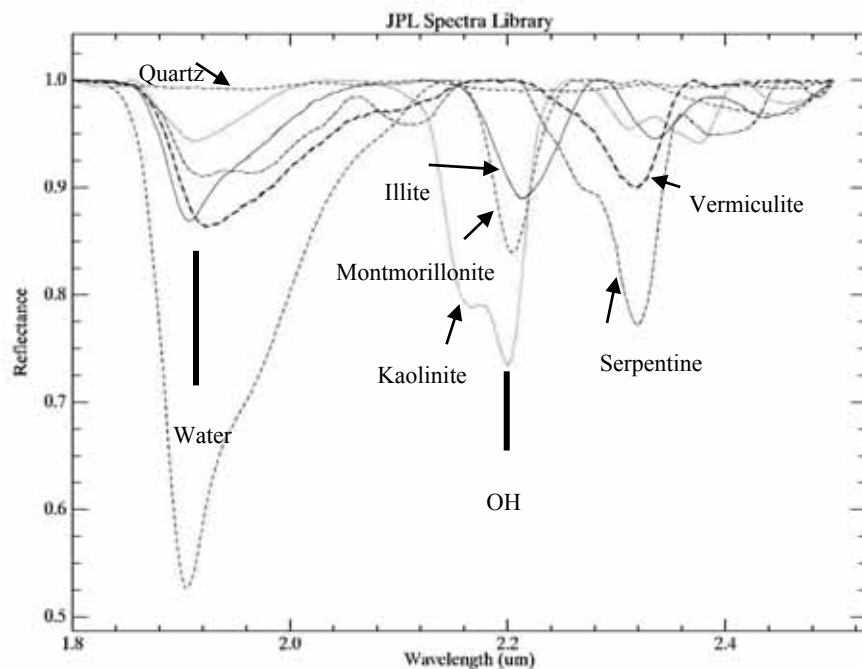


Fig 3 Continuum removed mineral spectra illustrating the separation between known minerals in the study areas (data from the Jet Propulsion Laboratory).

The diagnostic absorptions of the various minerals identified in the grape region are shown in Fig. 3 are spectra from the mineral spectral library (jpl1.sli) from the Jet Propulsion Laboratory (JPL, <http://asterweb.jpl.nasa.gov/specplib/>). Distinct absorption centers and doublets in the mineral absorptions can be compared by normalizing on the upper continuum of the spectrum (continuum removal)<sup>[36]</sup>. The

distinct spectral absorptions and widths of the diagnostic absorption bands for these minerals in the SWIR demonstrate that both the 1 nm field and 10 nm airborne spectrometers have sufficient spectral resolution for detection.

The initial analysis of the spectra was an ENVI spectral matching process. Library spectra were re-sampled to match the SWIR region in the range 1800 to 2500 nm. The results in spectral matching were good, and according to the USGS spectral library the best matches were with soil samples containing kaolinite/smectite clay minerals. However, the matching procedure did not adequately estimate the abundance of the minerals. One possible reason is spectral matching did not account for variation water content and its influence on the soil albedo and mineral absorption depths.

An alternate absorption mapping algorithm applied to the sample is the Modified Gaussian Model from Sunshine et al. [43]. This fitting algorithm finds the absorption centers of major absorptions for decomposing the spectrum to its elemental bond absorptions. The advantage of this technique is its ability to decompose individual bond absorption centers and strengths where adjacent absorptions combine overtones from the various ligand-metal combinations in the minerals. Spectral matching techniques require all the variations and combinations of band positions are contained the mineral library [44]. Unlike continuum removal, the spectrum is normalized at only one position, the maximum reflectance, and through additive overlapping absorptions set the spectrum shape. This algorithm performs well due to the convex shape in soil reflectance spectra. Multiple methods for choosing the appropriate continuum for separating individual absorptions has been suggested by [43], [45], [37] such as fitted polynomials and straight lines. Our modification is to add the inverted Gaussian from the SMGM to extend ultra-violet and SWIR regions to water fundamental near 200

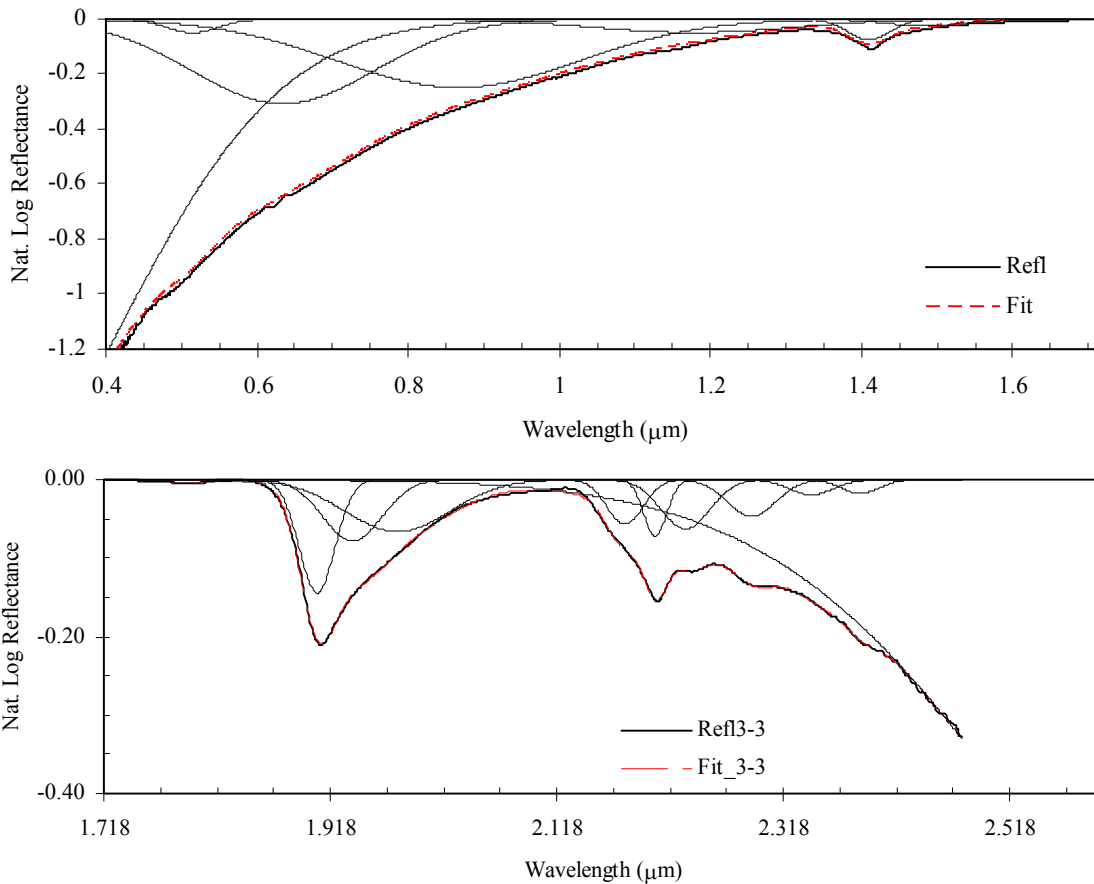


Fig. 4 Spectral de-convolution of the absorption features of sample 3-3 using the MGM. The normalized spectra (Refl) and the fitting (Fit), and the Gaussian distributions a) spectra in the visible, NIR and SWIR, and (c) spectra in the SWIR.

and 2800 nm. The inverted Gaussian functions require a minimum of 3 points to fit these major water absorptions before reaching the instrument limits at each end of the spectrum.

In Fig. 4 a and b, the spectrum of sample 3-3 is shown divided before and after the maximum reflectance point, and de-convolved to Gaussian absorptions beneath the normalized continuum using the MGM and SMGM continuum. The sum of overlapping absorptions is shown to fit the original spectrum. The RMSE of the fit was less than 0.001 reflectance for our samples. The algorithm starts the iterative fit on the transformed natural log reflectance using initial band centers determined using second derivative of the spectrum, and the addition of the 200 nm and 2800 nm water absorption centers to each end of the band center list. Through an iterative adjustment of the multiple inverted Gaussian function parameters until the predicted spectral shape is within the specified RMSE. From the absorption characteristics in the visible and near infrared regions are attributed to the  $\text{Fe}^{3+}$  vibration near the 550, 650 and 900 nm. Increased iron oxide is a diagnostic indicator for weathering of mineral with soil age. Vermiculite is found in the younger soil of this region.

The band centers and depths from the MGM/SMGM procedure were used in step-wise regression against the potassium fixation results to determine the best predictive absorptions; an unbiased approach to determining mineral bond to potassium fixation relationships. The resulting model with the few samples is promising, but not conclusive. Fixation values less than zero indicates the analysis released K, and insufficient range in fixation values creates a bimodal distribution. The significant band centers include 550 nm  $\text{Fe}^{3+}$ , 2190 nm Al-OH kaolinite, and 2320 nm Fe/MgOH. However, when the regression is based solely on the 2320 band assigned to vermiculite, and appears more reasonable, although the  $r^2$  drops to 0.36, but after reducing the samples to the geomorphology of known fixation, a model of 27 samples improved the predictive correlation to  $r^2 = 0.89$ . This geomorphology class is of the young, fine and coarse textured sediments, while non-fixing soils were generally on older low and high terraces and of volcanic parent material. The regression model for potassium fixing prediction on young sediments:

$$\text{k-fixation-potential} = 1780 - 383410 \cdot \text{BD}_{2320} \quad (1)$$

BD is the band depth of the de-convolved absorption at 2320 in natural log form.

### 2.3 In the field

In field spectroscopy of soil, on the surface or of the profile dug to two meters, the problems of mixed materials, instruments narrow field view, variation in bidirectional reflectance from soil surface (BRDF), atmospheric attenuation of the water bands, lack of sufficient spectral resolution in the SWIR to effectively discriminate mineral and organic matter types and abundance are always with us. However, soil water can be accounted for by measuring the fundamental and combination absorptions as indicators of the water content.

### 2.4 BSC moisture determining cover content.

In study of field spectral measurements of surface samples in Nevada, Mojave Desert, in southwestern continental USA, we determined that measurement of water bands was sensitive to variation in biological soil crust (BSC) cover from soil to estimate the amount of cover. In sparsely vegetated areas the microphytes, soil lichen and cyanobacteria growing on the soil surface protect from erosion, and increase the accumulation of soil organic matter, nutrient and water holding capacity to ameliorate the calcareous sandy soil conditions. These organisms also contribute substantially to carbon cycling when moist as demonstrated by other investigators<sup>[46][47]</sup>. In our research area, the predominant rugose gelatinous lichen *Collema* sp. and generally mixed with cyanobacteria, such as *Microcoleus* sp on gravel beds and sandy soil surfaces. In early spring, sparse grass and forbs are common on these hyperarid soils, in between the evergreen shrubs of Cresotebush (*Larrea tridentata*), and summer deciduous mountain white burro bush (*Ambrosia dumosa*), exposing more branch bark. Previous research determined the cover using NDVI and red + blue normalize difference index (Crust Index),<sup>[48]</sup> on sandy surface without other vegetation after moistening. Pursuing the concept that airborne or satellite image of the deserts is generally unavailable during the moist conditions, and there would be other green vegetation, we investigated a number of indexes to determine the amount of cover during the hyper dry states of summer.

We conducted spectral measurements of soil surfaces in endmember samples, field sample points, and of hyperspectral imagery of the research site. At the laboratory, samples of soil, lichen, cyanobacteria, and moss were moistened for 24 hours before drying in full summer sun. At ½ h intervals, the reflectance and weight measurements were made of the

endmembers during the solar window (2 h before and after solar noon, +/- 30 degrees of zenth) in the July temperatures of the California Central Valley where temperatures were above 40 °C. These endmember spectra were mixed with 5 % increments (with the addition of gravel bed spectra from the field) to create a synthetic image for analysis in IDL/ENVI (ITT Visual Solutions, Boulder, CO, USA). IDL script was used to smoothed the spectra with a Savitzky-Golay filter and determine the values for a large number of indexes, band depths, and absorption fitting algorithms for regressing in S-Plus statistical software (Insightful Corp. Seattle, WA, USA) against the known spectral mixture to determine the best candidate spectral indicators of BSC cover.

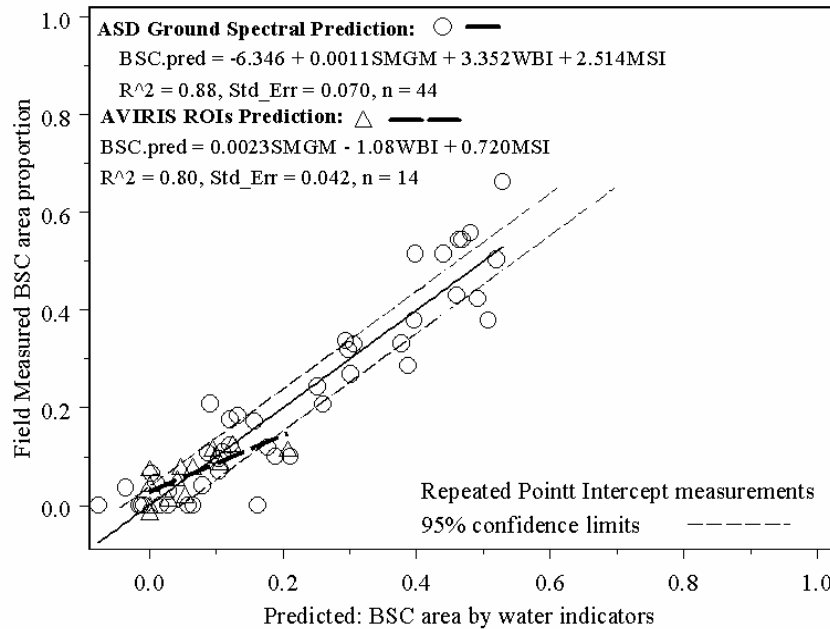


Fig. 5. Predictive models of BSC cover using field spectrometer and AVIRIS imagery compared to ground point intercept measured cover.<sup>[50]</sup>

in various significant combinations of narrow water indexes such as Water Band Index ( $WBI = R_{900}/R_{970}$ )<sup>[49]</sup>, Moisture Stress Index ( $MSI = R_{1600}/R_{820}$ )<sup>[30]</sup>, Normalized Difference Water Index ( $NDWI = R_{860} - R_{1240}/R_{860} + R_{1240}$ )<sup>[29]</sup> were found to be the best predictors.

Our research site was within the Mojave Global Change Facility within the US Department of Energy Nevada Test Site ([http://www.unlv.edu/Climate\\_Change\\_Research/MGCF/MGCF\\_index.html](http://www.unlv.edu/Climate_Change_Research/MGCF/MGCF_index.html)), a long-term undisturbed ecological research site simulating the effects of increased precipitation during the summer monsoons. At the sample points within the experimental plots, BSC cover were measured using the point intercept method for 121 points within the square 1/2 m that enclosed the ASD FieldSpect Pro full range spectrometer (Analytical Spectral Devices, Inc., Boulder, CO, USA) field of view (FOV). Points were measured repeatedly by different at least three observers at 11 sample sites to determine the method variance. For these field points, the SMGM, MSI and NDWI was the best significant combination of water band measurements with a linear regression predictive coefficient ( $R^2 = 0.88$ ; and RMSE of 7 %). In Fig. 5, the predictive model is generally within the confidence limits of the point-intercept measurements of the BSC in the FOV<sup>[50]</sup>.

On 5 November 2005, NASA Airborne Science Program flew the test site using their de Havilland Twin Otter aircraft. By extracting pixel spectra from location consistent with the point intercept measured sample points, the step-wise linear regression was applied to determine the best significant combination of water bands measures shown in Fig. 5. The BSC was predicted with SMGM, MSI, and NDWI with a predictive coefficient ( $R^2$ ) of 0.80 and RMSE of 4.2 %. Pixels with high NDVI values, indicating scrub content, were eliminated. These model coefficients were applied to the remaining pixel spectra to produce the BSC cover class map.

While vegetation indexes were successful in moist conditions, these indexes loss accuracy with decreasing gravimetric water content. Supporting the NDVI and photosynthesis relationship determined by Burgheimer et al.<sup>[47]</sup>. In the only consistent condition, the dry state, the vegetation indexes were poor predictors of cover. The water bands were highly predictive ( $R^2 > 0.97$ ) of the amount of crust in the synthetic mixtures using combinations of three water band measurements in the NIR and SWIR regions. Common to all the models was the Soil Moisture Gaussian Model (SMGM)<sup>[38]</sup> a technique of fitting an inverted Gaussian function to the log transformed SWIR spectra from the point of maximum reflectance to the fundamental water absorption at 2800 nm. The SMGM

The spatial extent of BSC can now be determined during the dry period to improve carbon exchange modeling during the moist warm periods and summer monsoon rain storms. Modeling carbon cycling in arid environments can be improved through the knowledge of the moisture conditions and rate of evapotranspiration rates of BSC. The limitations of required moisture for BSC activity and similar visible reflectance of soil and gravel and the ability to mask the vascular vegetation is overcome by modeling on the water content in soil surface. The variation of soil moisture was detectable in the natural desert scene after several weeks of extreme surface and air temperatures and low humidity.

### 3. CONCLUSION

Future activity and new ideas in image spectroscopy of soil should include modeling the soil spectrum using the basic principles of water absorptions and refraction, and reducing the amount of dependence on the statistical relationships.

### 4. REFERENCES

- [1] C. J. Tucker, "Red and photographic infrared linear combinations for monitoring vegetation.," *Remote Sensing of the Environment*, vol. 8, pp. 127 – 150, 1979.
- [2] A. R. Huete, "A Soil-Adjusted Vegetation Index (SAVI)," *Remote Sensing of Environment*, vol. 25, pp. 295-309, Aug 1988.
- [3] F. Baret, S. Jacquemoud, and J. F. Hanocq, "About the soil line concept in remote sensing.," *Advanced Space Research*, vol. 13, pp. 281-284, 1993.
- [4] H. Bach and W. Mauser, "Modelling and model verification of the spectral reflectance of soils under varying moisture conditions.," in *Proceedings IGARSS '94. 'Surface and Atmospheric Remote Sensing: Technologies, Data Analysis and Interpretation', IEEE International*, 1994, pp. 2354-2356.
- [5] M. F. Baumgardner, L. F. Silva, L. L. Biehl, and E. R. Stoner, "Reflectance properties of Soils," *Advances in Agronomy*, vol. 38, pp. 1-44, 1985.
- [6] T. L. Henderson, M. F. Baumgardner, D. P. Franzmeier, D. E. Stott, and D. C. Coster, "High dimensional reflectance analysis of soil organic matter.," *Soil Science Society of America Journal*, vol. 56, pp. 865-872, 1992.
- [7] E. R. Stoner and M. F. Baumgardner, "Characteristic variations in reflectance of surface soils.," *Soil Science Society of America Journal*, vol. 45, pp. 1161-1165, 1981.
- [8] S. A. Bowers and R. J. Hanks, "Reflection of radiant energy from soils.," *Soil Science*, vol. 100, pp. 130-138, 1965.
- [9] S. B. Idso, R. D. Jackson, R. J. Reginato, B. A. Kimball, and F. S. Nakayama, "The dependence of bare soil albedo on soil water content," *J. Appl. Meteor.*, vol. 14, pp. 109-113, 1975.
- [10] M. T. Yilmaz, E. R. Hunt, and T. J. Jackson, "Remote sensing of vegetation water content from equivalent water thickness using satellite imagery," *Remote Sensing of Environment*, vol. 112, pp. 2514-2522, 2008.
- [11] B.-C. Gao and A. F. H. Goetz, "Retrieval of Equivalent Water Thickness and information related to biochemical components of vegetation canopies from AVIRIS data," *Remote Sensing of Environment*, vol. 52, pp. 155-162, 1995.
- [12] G. S. Campbell, "Soil water potential measurement: An overview," *Irrigation Science*, vol. 9, pp. 265-273, 1988.
- [13] R. N. Clark, "Spectroscopy of rocks and minerals, and principles of spectroscopy.," in *Remote Sensing for the Earth Sciences: Manual of Remote Sensing, Third Ed., Vol 3.*, Third Edition ed. vol. 3, A. N. Rencz, Ed. New York: John Wiley & Sons, Inc, 1999, pp. 3-58.
- [14] E. Ben-Dor, J. R. Irons, and G. F. Epema, "Soil Reflectance.," in *Remote Sensing for the Earth Sciences: Manual of Remote Sensing*, 3 ed. vol. 3, A. N. Rencz, Ed. New York: John Wiley & Sons, Inc, 1999, pp. 111-188.
- [15] K. F. Palmer and D. Williams, "Optical properties of water in the near infrared.," *Journal of the Optical Society of America*, vol. 64, pp. 1107-1110, 1974.
- [16] G. M. Hale and M. R. Querry, "Optical constants of water in the 200-nm to 200-Mm wavelength region," *Applied Optics*, vol. 12, pp. 555-563, 1973.
- [17] J. L. Bishop, C. M. Pieters, and J. O. Edwards, "Infrared spectroscopic analyses on the nature of water in montmorillonite.," *Clays and Clay Minerals*, vol. 42, pp. 702-716, 1994.
- [18] R. E. Milliken and J. F. Mustard, "Quantifying absolute water content of minerals using near-infrared reflectance spectroscopy.," *Journal of Geophysical Research*, vol. 110, p. E12001, 2005.

- [19] F. Cariati, L. Erre, G. Micera, P. Piu, and C. Gessa, "Water molecules and hydroxyl groups in montmorillonites as studied by near infrared spectroscopy.," *Clays and Clay Minerals*, vol. 29, pp. 157-159, 1981.
- [20] B. Hapke, *Theory of Reflectance and Emittance Spectroscopy*. New York: Cambridge Univ. Press, 1993.
- [21] G. R. Hunt, "Spectral signatures of particulate minerals in the visible and near infrared," *Geophysics*, vol. 42, pp. 501-513, 1977.
- [22] E. Ben-Dor, Y. Inbar, and Y. Chen, "The reflectance spectra of organic matter in the visible near-infrared and short wave infrared region (400-2500 nm) during a controlled decomposition process," *Remote Sensing of Environment*, vol. 61, pp. 1-15, 1997.
- [23] W. H. Gardner, "Water Content," in *Methods of soil analysis. Part 1. Physical and mineralogical methods. 2nd ed.* vol. 9, A. Klute, Ed.: Agronomy, 1986, pp. 493-544.
- [24] M. Persson, "Estimating surface soil moisture from soil color using image analysis," *Vadose Zone Journal*, vol. 4, pp. 1119-1122, 2005.
- [25] D. F. Post, A. Fimbres, A. D. Matthias, E. E. Sano, L. Accioly, A. K. Batchily, and L. G. Ferreira, "Predicting soil albedo from soil color and spectral reflectance data," *Soil Science Society of America Journal*, vol. 64, pp. 1027-1034, 2000.
- [26] E. L. Skidmore, J. D. Dickerson, and H. Schimmeelpfenning, "Evaluating surface-soil water content by measuring reflectance.," *Soil Science Society of America Proceedings*, vol. 39, pp. 238-242, 1975.
- [27] J. H. Everitt, D. E. Escobar, M. A. Alaniz, and M. R. Davis, "Using multispectral video imagery for detecting soil surface conditions," *Photogrammetric Engineering and Remote Sensing*, vol. 55, pp. 467-471, 1989.
- [28] H. B. Musick and R. E. Pelletier, "Response of some Thematic Mapper band ratios to variation in soil water content.," *Photogrammetric Engineering and Remote Sensing*, vol. 52, pp. 1661-1668, 1986.
- [29] B.-c. Gao, "NDWI--A normalized difference water index for remote sensing of vegetation liquid water from space," *Remote Sensing of Environment*, vol. 58, pp. 257-266, 1996/12 1996.
- [30] J. Hunt, E. Raymond and B. N. Rock, "Detection of changes in leaf water content using Near- and Middle-Infrared reflectances," *Remote Sensing of Environment*, vol. 30, pp. 43-54, 1989/10 1989.
- [31] W. Liu, F. Baret, X. Gu, Q. Tong, L. Zheng, and B. Zhang, "Relating soil surface moisture to reflectance.," *Remote Sensing of Environment*, vol. 81, pp. 238-246, August 2002 2002.
- [32] W. Liu, F. Baret, X. Gu, B. Zhang, Q. Tong, and L. Zheng, "Evaluation of methods for soil surface moisture estimation from reflectance data.," *International Journal of Remote Sensing*, vol. 24, pp. 2069-2083, 2003.
- [33] R. C. Dalal and R. J. Henry, "Simultaneous determination of moisture, organic carbon and total nitrogen by near infrared reflectance spectroscopy.," *Soil Science Society of America Journal*, vol. 50, pp. 120-123, 1986.
- [34] J. A. M. Demattê, A. A. Sousa, M. C. Alves, and M. R. Nanni, "Determining soil water status and other soil characteristics by spectral proximal sensing.," *Geoderma*, vol. 135 pp. 179-195, 2006.
- [35] D. B. Lobell and G. P. Asner, "Moisture effects on soil reflectance," *Soil Science Society of America Journal*, vol. 66, pp. 722-727, May-June 2002 2002.
- [36] R. N. Clark and T. L. Roush, "Reflectance spectroscopy: Quantitative analysis techniques for remote sensing applications," *Journal of Geophysical Research*, vol. 89, pp. 6329-6340, 1984.
- [37] R. E. Milliken and J. F. Mustard, "Estimating the water content of hydrated minerals using reflectance spectroscopy: I. Effects of darkening agents and low-albedo materials," *Icarus*, vol. 189, pp. 550-573, 2007.
- [38] M. L. Whiting, L. Li, and S. L. Ustin, "Predicting water content using Gaussian model on soil spectra.," *Remote Sensing of Environment*, vol. 89, pp. 535-552, 17 Feb 2004 2004.
- [39] R. E. Milliken and J. F. Mustard, "Observations and modeling of the absorbed water in montmorillonite with reflectance spectroscopy.," in *Lunar and Planetary Science 34th Annual Conference*, League City, TX, 2003.
- [40] D. J. Mulla, P. F. Low, and C. B. Roth, "Measurement of the specific surface area of clays by internal reflectance spectroscopy," *Clays and Clay Minerals*, vol. 33, pp. 391-413, 1985.
- [41] B. Peacock and P. Christensen, "Potassium and boron fertilization in vineyards.," *Pub. #NG1-96. (newsletter)*, University of California Cooperative Extension, Tulare Co. Tulare, CA. <http://cetulare.ucdavis.edu/pubgrape/ng196.htm> 1996.
- [42] G. W. Thomas, "Exchangeable cations.," in *Methods of soil analysis: Part 2. Chemical and microbiological properties, ASA Monograph Number 9*: A.L. Page et al., 1982, pp. 159-165.
- [43] J. M. Sunshine, C. M. Pieters, and S. F. Pratt, "Deconvolution of mineral absorption bands - an improved approach," *Journal of Geophysical Research-Solid Earth and Planets*, vol. 95, pp. 6955-6966, May 10, 1990 1990.

- [44] J. F. Mustard and J. M. Sunshine, "Spectral analysis for Earth science: Investigations using remote sensing data.," in *Remote Sensing for the Earth Sciences: Manual of Remote Sensing, Third Ed., Vol 3.*, Third Edition ed. vol. 3, A. N. Rencz, Ed. New York: John Wiley & Sons, Inc, 1999, pp. 251-306.
- [45] T. Hiroi, C. M. Pieters, and S. K. Noble, "Improved scheme of modified Gaussian deconvolution for reflectance spectra of lunar soils.," in *Lunar and Planetary Science 34th Annual Conference*, League City, TX, 2000.
- [46] O. L. Lange, J. Belnap, and H. Reichenberger, "Photosynthesis of the cyanobacterial soil-crust lichen *Collema tenax* from arid lands in southern Utah, USA: role of water content on light and temperature responses of CO<sub>2</sub> exchange," *Functional Ecology*, vol. 12, pp. 195-202, 1998.
- [47] J. Burgheimer, B. Wilske, K. Maseyk, A. Karnieli, E. Zaady, D. Yakir, and J. Kesselmeier, "Ground and space spectral measurements for assessing the semi-arid ecosystem phenology related to CO<sub>2</sub> fluxes of biological soil crusts," *Remote Sensing of Environment*, vol. 101, pp. 1-12, 2006.
- [48] A. Karnieli, "Development and implementation of spectral crust index over dune sands," *International Journal of Remote Sensing*, vol. 18, pp. 1207-1220, 1997.
- [49] J. Peñuelas, J. Piñol, R. Ogaya, and I. Filella, "Estimation of plant water concentration by the reflectance Water Index (R900/ R970)." *International Journal of Remote Sensing*, vol. 18, pp. 2869-2875, 1997.
- [50] M. L. Whiting and S. L. Ustin, "Mapping of desert biological soil crust using hyperspectral water bands.," in *6th EARSeL SIG IS Workshop, Imaging Spectroscopy: Innovative tool for scientific and commercial environmental applications*, Tel-Aviv, Israel, 2009.